

Self-Assembly

Using Hydrogen Bonds to Direct the Assembly of Crowded Aromatics

Mark L. Bushey, Thuc-Quyen Nguyen, Wei Zhang, Dana Horoszewski, and Colin Nuckolls*

Keywords:

aromaticity · hydrogen bonds · molecular recognition · nanotechnology · self-assembly

This Minireview details the design, synthesis, and self-assembly of a new class of crowded aromatics that form columnar superstructures. The assembly of these subunits produces helical and polar stacks, whose assembly can be directed with electric fields. In concentrated solutions, these self-assembled helical rods exhibit superhelical arrangements that reflect circularly polarized light at visible wavelengths. Depending on the side chains employed, spin-cast films yield either polar monolayers or isolated strands of molecules that can be visualized with scanning probe microscopy. Also detailed herein are methods to link these mesogens together to produce monodisperse oligomers that fold into defined secondary conformations.

1. Introduction

Self-assembly is a powerful tool to create novel materials with emergent or amplified properties.^[1] Discotic liquid crystals are one such self-assembled system.^[2] This relatively new class of liquid crystalline compounds, discovered in 1977 by Chandrasekar and co-workers,^[3] is composed of arrayed, one-dimensional columns formed through self-assembly. The constituent stacks have been likened to molecular-scale wires because the interior of the column consists of cofacially stacked π faces while its exterior is surrounded by an insulating, hydrocarbon wrapper.^[4] This arrangement of the aromatic cores has endowed these liquid crystalline phases with useful electronic and optic properties.^[5]

For traditional discotics the affinity between the subunits is low due to the poor electrostatic attraction between the electron rich π surfaces.^[6] Strategies that utilize metal–ligand interactions,^[7] recognition of polymer strands,^[8] electrostatic complementarity between π faces,^[9] and hydrogen bonds^[10]

have yielded columnar assemblies that are held together more strongly.

This Minireview details the assembly characteristics of a new class of columnar materials that are held together with hydrogen bonds.^[11] The core is a hexasubstituted aromatic (1

and 2 in Figure 1) consisting of three amides in the 1,3,5-positions that are flanked by substituents other than hydrogen

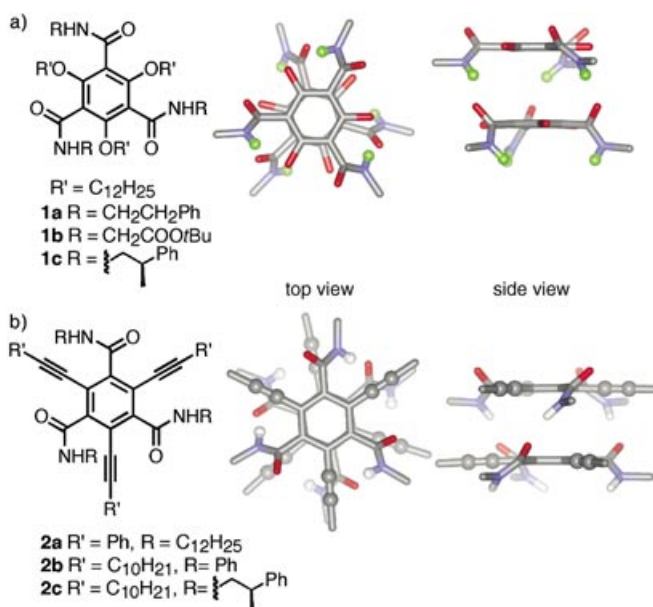


Figure 1. Crowded aromatics and their energy-minimized molecular models. Side chains and hydrogen atoms have been removed to clarify the view.

[*] M. L. Bushey, T.-Q. Nguyen, W. Zhang, D. Horoszewski, Prof. C. Nuckolls
 Department of Chemistry
 Columbia University
 New York, NY 10027 (USA)
 Fax: (+1) 212-932-1289
 E-mail: cn37@columbia.edu

at each of the remaining positions. There are four sections below detailing the self-assembly characteristics of **1** and **2**: 1) The general design and synthesis of this new class of mesogens. 2) The synthesis of small but informationally rich, chiral subunits that stack to form helical rods. The assembly of these rods can be directed by electric fields. In concentrated solutions, a superhelix is formed that reflects circularly polarized light at visible wavelengths. 3) Monitoring the assembly of these mesogens in monolayer films has yielded films with two orientations controlled by the substituents in the side chain. In one surface conformation a two-dimensional sheet results that is macroscopically polar. In the other orientation on the surface, one-dimensional π stacks result that are only a few molecules wide but microns in length. 4) Differentiation of the substituents on each of the amides creates a new class of monodisperse, step-growth oligomers from these highly functionalized mesogens. When appropriate linkers are incorporated into these oligomers, they fold into defined secondary superstructures.

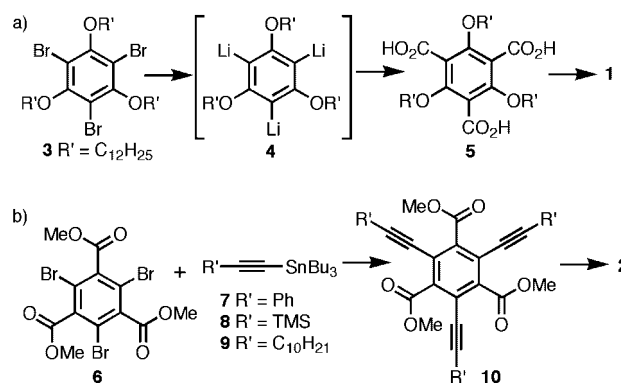
2. General Design, Synthesis, and Bulk Assembly

The design of the molecules in Figure 1 was based on the large number of examples of benzene and cyclohexyl rings that are cofacially stacked with the aid of hydrogen bonds.^[10] Particularly salient are the crystal structures of benzene^[10d,f] and cyclohexane^[10d,e] that are substituted at their 1,3,5-positions with amides. These structures and similar ones inferred from columnar liquid crystals studied by the groups of Matsunaga^[10a] and Meijer^[10b] reveal a one-dimensional stacked structure held together by amide hydrogen bonds. For the molecules in Figure 1, the design principle explored was how to use the flanking alkoxy groups for **1** and alkynyl substituents for **2** to force the amides out of the plane of the central aromatic ring and into a conformation that is predisposed to form three intermolecular hydrogen bonds. Shown in Figure 1 are the energy-minimized dimeric models for both **1** and **2**.^[11a,b,e] From models, the size of the flanking substituent determines the angle of twist for the amide out of the central ring plane and consequently modulates the distance between adjacent benzene rings. The center-to-center distance between the benzene rings is about 3.8 Å for **1** and about 3.6 Å for **2**, thus reflecting the relative sizes of the

alkoxy and the alkynyl substituents. A second interesting feature of the models in Figure 1 is that each of the subunits has a permanent dipole moment, whose direction is perpendicular to the ring plane. Therefore, as the molecules stack, the dipoles could sum to yield columns that have a macroscopic dipole moment, similar to the moment that is seen for some metallomesogens and conical liquid crystals.^[12] In principle, these polar columns could be useful not only in understanding how polar properties emerge on the nanoscale but also for creating small-scale piezoelectric, pyroelectric, and ferroelectric objects.

2.1. Synthesis

Because **1** and **2** were unknown before the studies below were initiated, a versatile synthesis was required to provide a large number of derivatives to understand the structure–property relationships. Moreover, the highly substituted nature of these aromatics provides a test bed for developing new synthetic methodology. For **1**, the key to their synthesis was a triple lithium–halogen exchange with **3** to produce the trilitio derivative **4** (see Scheme 1). Quenching **4** with carbon



Scheme 1. a) Synthesis of **1**. b) Synthesis of **2**.

dioxide or its synthetic equivalent provides these substituted trimesic acid derivatives.^[11a] For the alkynyl substituted derivatives (**2**), the key step was a Farina-modified, Stille coupling of an alkynyl stannane with a 1,3,5-tribromo triester of benzene.^[11e] For both series, multiple grams of a versatile trisacid chloride can be synthesized. These acid chlorides can then be treated with a variety of readily available amines to yield the trisamides shown in Figure 1.

2.2. Assembly in Bulk

Of the two series, **1** is the more heavily studied. Their assembly in bulk is deduced from a confluence of experiments that include synchrotron X-ray diffraction, polarized-light microscopy, infrared spectroscopy, and differential scanning calorimetry.^[11a,b] The essential conclusion from these experiments is that the assembly process is dominated by the size and polarity of the amide side chains. For example, when the



Colin Nuckolls was born in 1970 at Lakenheath RAF (UK) and received his Ph.D. in 1998 (Columbia University, New York). After a postdoc at The Scripps Research Institute, he returned in 2000 to Columbia as an Assistant Professor of Organic Chemistry. He studies the design, synthesis, and assembly of electronic materials on molecular length scales. He has been awarded The NSF CAREER Award (2003), The Beckman (2002) and The Dupont Young Investigator Awards (2002), and the NYSTAR James D. Watson Investigator Award (2002). He is a founding member of the Columbia University Nanoscience Center.

amide substituents are relatively small such as the phenethyl substituents of **1a**, the material assembles into extremely regular cylinders that are hexagonally packed into millimeter-scale domains. When the phenethyl side chain is exchanged for $\text{CH}_2\text{COO}t\text{Bu}$ (**1b**; Figure 1), the material is no longer able to stack into perfect cylinders and compensates by positioning the subunits either canted or offset. These misalignments produce a distorted hexagonal lattice for **1b**. Further magnifying this trend, when the amide substituent is now changed $\text{CH}(\text{CH}_3)\text{COO}t\text{Bu}$ (now made even bulkier!), there is no discernable mesomorphism in bulk samples.

Although there are less data, it appears that the substituents on the side chains of **2** have less influence on the mesomorphism.^[11e] Each of the derivatives shown in Figure 1b (**2a–c**), as well as others, displays a hexagonal arrangement of cylinders. This difference in stacking propensity between **1** and **2** is likely to be the result of the gearlike arrangement of side chains in **1** that is lacking in **2** due to the linearity of the alkynyl substituent.

3. Transfer of Chiral Information

Chiral centers incorporated into the amide side chains have tremendous influence on the mesomorphism observed for derivatives of **1**.^[11b] Shown in Figure 2a is the polarized light micrograph from **1c** that is optically pure and in

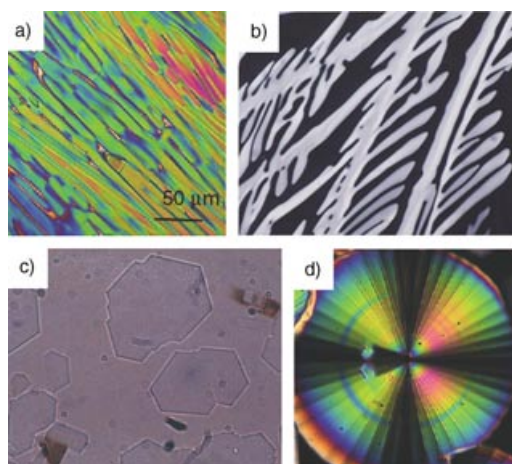


Figure 2. a) Polarized-light micrograph of optically active $(-)\text{-1c}$ cooled from its clearing point; b) polarized-light micrograph of optically active **1c** between two sheets of indium tin oxide on glass electrodes spaced by $5\ \mu\text{m}$, $0\ \text{V}$ applied; c) as in **2b**, polarizer removed, $30\ \text{V}$ applied; d) Polarized-light micrograph of racemic **1c** cooled from its clearing point.

Figure 2d from **1c** that is racemic. These micrographs in combination with synchrotron X-ray diffraction experiments show that while both are hexagonally arranged into columns with similar lattice spacings they have drastically different phase behavior. These experiments and others outlined below indicate that the optically active material is in a columnar liquid-crystalline phase, while the racemate is in a soft or plastic crystalline phase. The spherulitic domains of the

racemate are the same as those from **1a**, a compound that lacks the angular methyl group. The role of these remote chiral centers in directing the assembly is extremely subtle as the clearing temperatures, lattice spacings, IR stretches, and enthalpies of transition are all very similar for either $(-)\text{-1c}$ or $(\pm)\text{-1c}$. In models of **1c** the methyl and the phenyl substituents are able to make positive contacts only when the material is racemic. This could provide the chiral information transfer between the subunits of the stacks.

3.1. Electrostatic Self-Assembly

The presence of this liquid-crystalline phase in optically active $(-)\text{-1c}$ allows for the testing of whether the columnar assembly can be directed by the application of electric fields.^[11b] The micrographs in Figure 2b and 2c were recorded as $(-)\text{-1c}$ was cooled from its isotropic liquid into its mesophase while sandwiched between ITO coated glass plates separated by $5\ \mu\text{m}$. When no electric field is applied, the material is brightly birefringent with the columnar axes parallel to the surface (Figure 2b). When an electric field is applied, the material becomes optically isotropic, and only when the polarizer is removed can the micron-size polygons, shown in Figure 2c, be visualized. The corners on these polygons have perfect 120° angles indicative of the hexagonal symmetry of the underlying lattice. The racemic materials show no such effect, as spherulitic domains, like those in Figure 2d, result with or without an electric field. The implication is that for the optically active material, electric fields are able to direct the assembly of the columns and their dipoles. Typically the growth of discotic mesophases is more easily affected with magnetic fields,^[13] rather than electric fields, because of the magnetic anisotropy of the standard aromatic cores. For these crowded mesogens, electric fields are efficacious due to the head-to-tail hydrogen bonds in these mesogens endowing the columns with polarity. Although the trisamides of Meijer and co-workers have been shown to switch in electric fields, they do so only when diluted with solvent.^[14] Presumably, these diluted mesogens are in a lyotropic nematic phase and switch because of a dielectric response. The difference in the mechanism for these lyotropics and the one operating for optically active **1c** may be related to the interplay between chirality and polar properties that can only emerge in the neat material. This notion is magnified by results on the trisalkynes that show switching half-times in the order of microseconds and signatures of polar ordered materials when they are prepared optically active.^[11e]

3.2. Helices and Superhelices in Solution

Molecular models such as the one shown in Figure 3a reveal that as the molecules stack, three helices of hydrogen bonds emerge around the exterior of the columns,^[11b] similar to that seen for the unsubstituted 1,3,5-triamides of benzene.^[10d,f] Because the amide rotation is less than 90° out of the plane of the benzene ring, the molecules are only

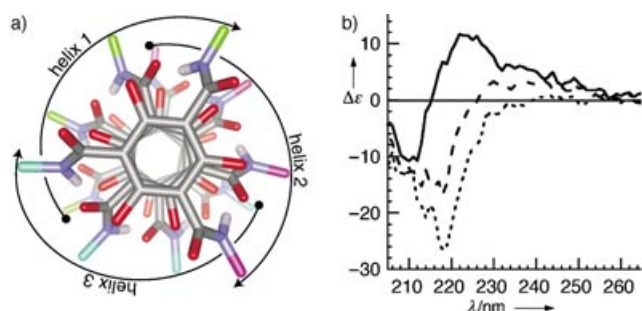


Figure 3. a) Molecular model of four molecules of **1** showing the emergence of three helices of hydrogen bonds around the exterior; b) Circular dichroism (CD) spectra in solution for **1c** in hexanes with varying amounts of methylene chloride (— 15%, - - - - 20%, and - - - - 30%).

complementary with all amides in the same rotational phase. The contact between the six substituents on the benzene ring means that it is possible to bias the gearing of the substituents in one direction or the other, which could be controlled by the chirality in the side chain. Also, the chiral centers in **1c** can influence the winding of these helices. The difference in packing of helices derived from either the racemic or optically active molecules could provide a mechanism for the two materials to behave so differently.^[15]

Experimental evidence for helicity in columns from **1c** is shown in the CD spectra in Figure 3b. In solvents that cannot effectively compete for the hydrogen bonds, the molecules aggregate, and the amide side chain chromophores in adjacent molecules come close enough to be excitonically coupled, displaying a Cotton effect as in Figure 3b. Similar effects have been seen for other columnar systems with chiral centers in the side chains.^[16] In more competitive solvents, the split CD disappears because the hydrogen bonded assembly is broken, and the chromophores are now isolated from each other. The CD of the isolated molecules reflects its intrinsic chirality but lacks the splitting due to excitonic coupling.

In concentrated hydrocarbon solutions, derivatives of **1** and **2** display a wide range of lyotropic mesomorphism.^[11b] When **1b**, which displays a nematic texture on its own in dodecane solvents, is mixed with (–)-**1c**, the solutions reflect circularly polarized light in visible wavelengths. This behavior is diagnostic of a well-known assembly motif in helically wound polymers to form what is termed a cholesteric liquid-crystalline phase.^[17–21] In this mesophase the helices pack next to one another with defined twist angles as shown in Figure 4c.

The wavelength that cholesterics reflect circularly polarized light is a useful property for a diversity of applications ranging from temperature sensing^[22] to lasing.^[23] For the **1a**/ (–)-**1c** mixture this wavelength can be easily tuned by the ratio of the components, temperature, and amount of solvent. For the composition that is shown in the micrographs obtained with polarized light in Figure 4a and b, the wavelength of reflected circularly polarized light is in the visible region of the spectrum, which expands from green at 40 °C to red at 60 °C. Although ubiquitous in rodlike helical polymers,^[16–20] this type of liquid crystalline phase is not observed

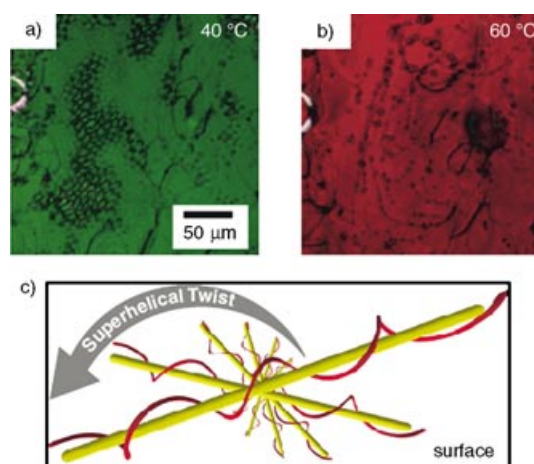


Figure 4. Selective reflection of circularly polarized light from a mixture of (–)-**1c**, **1b**, and dodecane: a) green at 40 °C; b) red at 60 °C; c) schematic of the cholesteric superhelix.

in classic discotics and other self-assembled columnar structures.^[15a] Presumably, the hydrogen bonds provide a higher association in the stacking direction and thereby form a sizable column in solution while the chiral side chains provide the helicity. In essence, the aggregates in solution act as noncovalent polymers.^[24]

4. Organization in Monolayer Films

4.1. Polar monolayers

One feature of the assembly of derivatives of **1** and **2** that is potentially useful has to do with their polar properties and how they develop on the nanoscale. To investigate the assembly and polarity of **1** and **2** on these length scales, conditions were found to produce films that have less than a monolayer of coverage on highly ordered pyrolytic graphite substrates through spin casting.^[11c] The topography and polarity of these films can be measured simultaneously by using atomic force microscopy (AFM) and electrostatic force microscopy (EFM).^[25] For **1b**, the height of the overlayer shown in Figure 5a is about 0.5 nm, thus indicating that the aromatic rings are parallel to the surface. The important finding shown in Figure 5a and b is that the AFM and EFM images look essentially the same, which implies that the film has a universal net negative charge. The EFM signal is a convolution of the molecular charge due in large part to charge transfer from the substrate and/or a perpendicular, permanent dipole moment. Because of the partial positive charge on the amide proton coupled with its out-of-plane conformation, an N–H/ π interaction with the graphite substrate as shown in Figure 5c could result.^[26] Effectively, the surface could serve to orient the amide substituents and thereby direct the molecular dipoles.^[27] Electron transfer from the graphite to the monolayer could also be a contributor to the EFM signal.

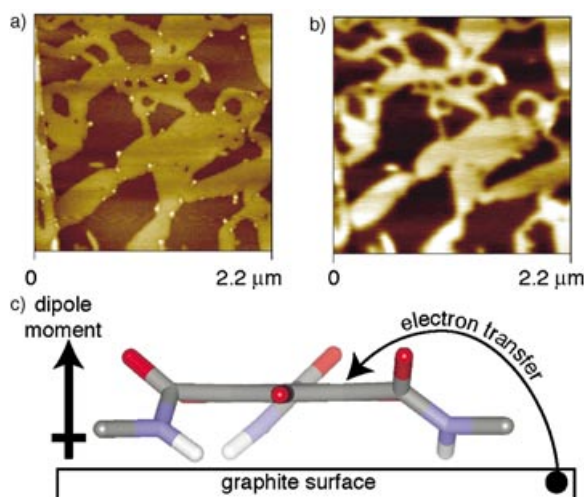


Figure 5. a) $4.8 \mu\text{m}^2$ AFM height image; b) EFM 1ω image of the same film. c) Dipole and electron transfer in thin films of **1b**. Reprinted, with permission, from reference [11c]. Copyright 2002 The American Chemical Society.

4.2. Isolated Stacks

Remarkably, the opposite surface orientation, in which the columns align parallel to the surface (Figure 6d), is adopted for all other derivatives shown in Figure 1 (**1a**, **1c**, and **2a–c**) and others tested that form hexagonal arrangements in bulk. The dominant feature in the AFM micrographs (Figure 6) is the large number of molecular-scale, fibrous

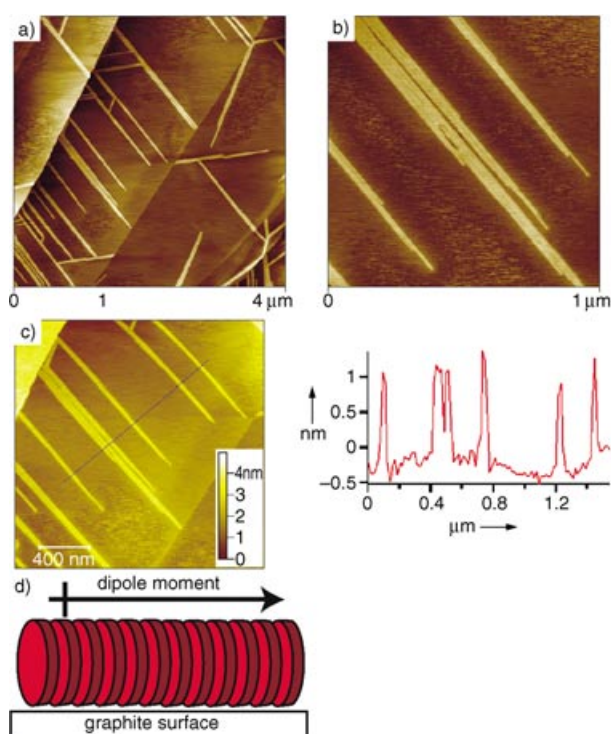


Figure 6. AFM images of **1c** on graphite at various scan sizes: a) $16 \mu\text{m}^2$, b) $1 \mu\text{m}^2$, c) The cross section profile of a fiber. d) Schematic of orientation of **1c** on graphite substrates. Reprinted, with permission, from reference [11c]. Copyright 2002 The American Chemical Society.

regions. Each of the striations within a fiber is about 2 nm in diameter (Figure 6b) and the height of these features is 1.80 ± 0.22 nm (Figure 6c). These values correlate well with the 1.8 nm column spacing measured from bulk synchrotron X-ray diffraction.^[11a,b] EFM analysis of these stacks reveals that they have essentially no measurable dipole or charge, which is consistent with the dipole moment of the column being parallel to the surface (Figure 6d).

There are few examples of similar molecular-scale fibers from columnar mesophases.^[28] Possibly, one-dimensional structures do not form for typical discotic mesogens because the relatively weak π -stacking forces that hold the column together are nearly equaled in energy by the numerous van der Waals contacts between alkyl side chains giving rise to two-dimensional sheets.^[29] For the derivatives in Figure 1, the self-association in the stacking direction due to the hydrogen bonds now outweighs these van der Waals contacts between columns, and individual stacks can be isolated. Ongoing experiments involve the use of scanning tunneling microscopy to determine the local structure in these strands.

It is important to note that the propensity to stack the aromatic cores face-on as for **1b** and edge-on as for **1c** elucidated from the AFM/EFM studies above mirrors the same propensity for assembly in bulk: **1b** has a homeotropic alignment while **1c** has a planar arrangement of columns.^[11a,b] What is the origin of the difference in orientation between **1b** and **1c** in monolayer films and in bulk? One possible explanation has to do with the difference in association between **1b** and **1c**. **1c** readily self-assembles to form strands that orient their long axes parallel to the substrate. The stacking of **1b** is now weakened owing to the sterically demanding side chains, and the interaction with the surface dominates, giving rise to the face-on conformation at the interface. Possibly this monolayer forms also in bulk samples of **1b** and serves as a surface template to direct the assembly of subsequently stacked mesogens.

5. Folded Oligomers

One unique feature of these crowded aromatics is their highly substituted core that contains two different types of side chains. If each of the amides could be differentially substituted, then subunits could be linked together to form monodisperse step-growth oligomers.^[11d] Because of the helicity of the amide hydrogen bonds in these stacks shown in Figure 3a, oligomers could have a defined secondary structure similar to that of α -helically wound peptides, thus

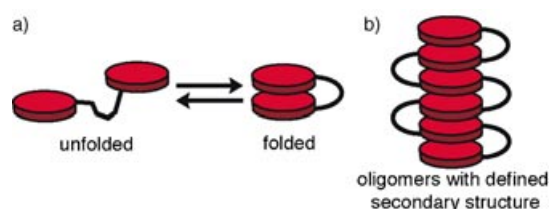
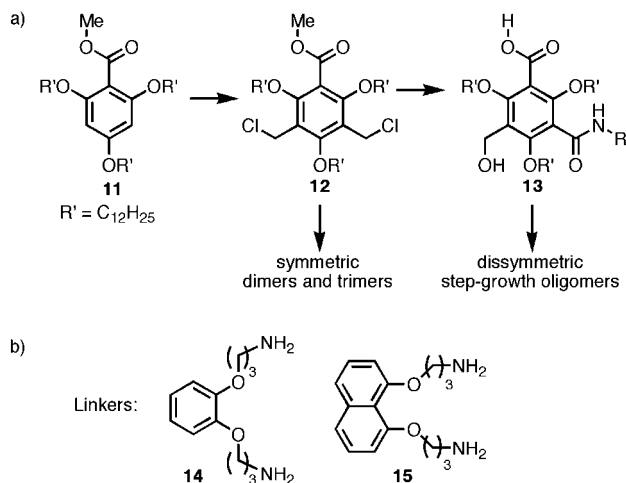


Figure 7. a) Schematic of linking two crowded aromatics to study the process of folding and unfolding in dimers; b) Schematic of a monodisperse oligomer that folds into a defined conformation.

forming a new class of foldamers shown in Figure 7b.^[30] The initial objective was to develop a synthetic methodology that would allow each of the amides to be individually substituted and to see what types of linkers produced folded conformations as shown in Figure 7a.

A high yielding and large-scale synthesis of derivatives of **1**, in which each of the amides can be individually addressed



Scheme 2. a) Synthesis of differentially substituted triamides. b) Linkers used for oligomer construction.

(Scheme 2), was recently completed and has allowed the synthesis of not only dimers but also oligomers of defined length such as in Figure 7b.^[11d] The key to the synthesis was the finding that the tetrasubstituted aromatic **11** could be chloromethylated to install the final two carbon atoms on the hexasubstituted core of **12**. Through a multistep sequence of hydrolysis, oxidation, and coupling, symmetrical dimers (**16**, **17**, and **18** in Figure 8) and trimers can be synthesized from **12**. After the conversion of **12** to its diacetoxymethyl derivative, one of the acetates could be saponified to yield the fully differentiated monomer **13**. This monomer could be used to synthesize unsymmetrical dimers, trimers, and higher oligomers.

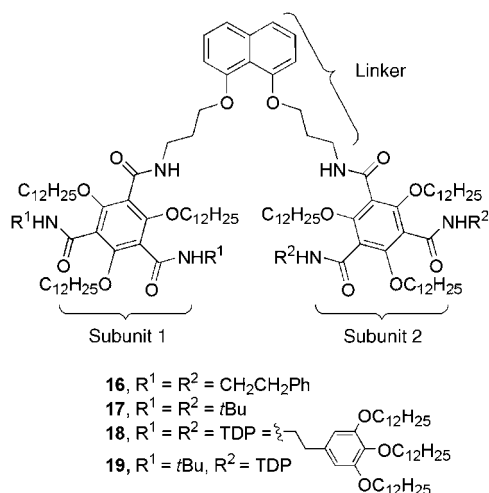


Figure 8. Homo- and heterodimers synthesized with the C-shaped 1,8-naphthyl linker. Reprinted, with permission, from reference [11d]. Copyright 2003 The American Chemical Society.

5.1. Folding in Dimers

Crucial to observing folding of these oligomers in solution was the employment of C-shaped linkers such as the catechol-based linkers or the 1,8-naphthyl-based linkers shown in Scheme 2b.^[11d] This new folding motif is so robust that even dimers have secondary structure in solution. A signature of the folded conformation in dimers is the about 1 ppm downfield shifts in the amide N–H ¹H NMR resonances. Unsymmetrical dimers have numerous through-space NOE couplings indicative of the folded conformation in Figure 7a. Linear aromatic and alkyl linkers do not exhibit such self-folding properties, thus showing the importance of preorganizing the system for intramolecular contacts. In addition to the linker, the side chains in these oligomers are also critical for the secondary structure to emerge in solution. As with the monomers shown in Figure 1, the phenethyl side chains and the substituted phenethyl side chains proved useful in allowing the subunits to fold. The *tert*-butyl amide side chains can be incorporated into the terminal subunit and block head-to-tail aggregation of these oligomers above millimolar concentrations.

5.2. Folding in Higher Oligomers

By using the highly solubilizing tris(dodecyloxy)phenethyl (TDP) side chains with the *tert*-butyl side chains in the terminal subunit has allowed higher oligomers to be synthesized. Shown in Figure 9 is the structure, ¹H NMR spectrum, and through space NOE couplings observed in a CD₂Cl₂ solution. The oligomer adopts a well-defined columnar structure. More recently, hexamers have been synthesized and their phase behavior and assembly in thin films is being studied. Due to the highly substituted nature of these columns it should be possible to write chemical information into these

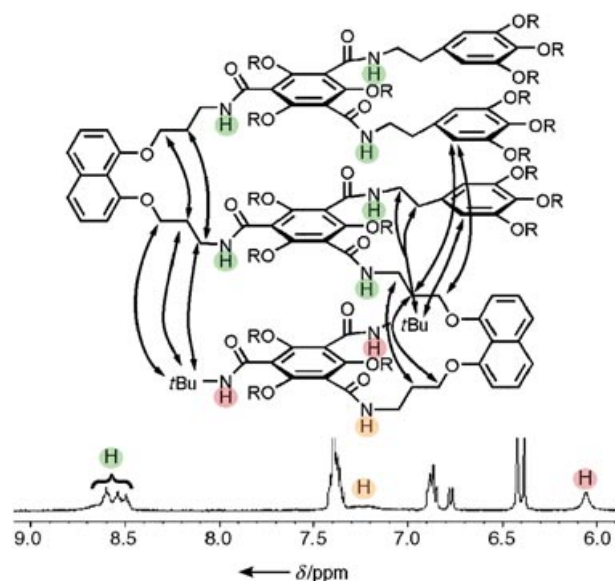


Figure 9. NOE couplings and ¹H NMR spectrum for a trimer (1 mM in CD₂Cl₂, 303 K, R = C₁₂H₂₅). Reprinted, with permission, from reference [11d]. Copyright 2003 The American Chemical Society.

structures that would encode their assembly into higher order structures.

6. Summary and Outlook

This Minireview details the design, synthesis, and self-assembly of a new class of molecules that form columnar superstructures. The structures of **1** and **2** are unique synthetic targets owing to the highly substituted central benzene ring. The assembly of these subunits produces helical and polar stacks whose assembly can be directed with electric fields. These helical rods also exhibit cholesteric mesophases in concentrated solutions, a unique mesomorphism for self-assembled columnar mesogens. Spin casting of films of **1b** produces polar monolayers that can be visualized with AFM and EFM. The understanding of how the polarity in this initial layer is transferred to subsequently stacked molecules is a necessary goal to rationalize how to create spontaneously polar materials. Monolayers of **1c** form isolated stacks that are microns in length but only a few molecules wide. Measurement of electrical and polar properties on these strands is an ongoing challenge for this new class of nanoscale materials. Also detailed above are methods to link these mesogens together to produce monodisperse oligomers of **1** that fold into defined secondary conformations. Ongoing experiments are aimed at investigating the self-assembly of these oligomers into higher-order aggregates.

We acknowledge the support from numerous collaborators, coworkers, and colleagues that made these studies possible. We acknowledge primary financial support from the Chemical Sciences, Geosciences and Biosciences Division, Office of Basic Energy Sciences, US D.O.E. (no. DE-FG02-01ER15264), US National Science Foundation CAREER award (no. DMR-02-37860), and the Nanoscale Science and Engineering Initiative of the National Science Foundation under NSF Award Number CHE-0117752 and by the New York State Office of Science, Technology, and Academic Research (NYSTAR). CN thanks the Beckman Young Investigator Program (2002), the NYSTAR J. D. Watson Investigator Program (2003), and the Dupont Young Investigator Program (2002) for support. MLB thanks the ACS Division of Organic Chemistry for a graduate fellowship sponsored by Bristol-Myers Squibb.

Received: July 9, 2003

Revised: November 13, 2003

Published Online: September 16, 2004

- [1] a) J.-M. Lehn, *Supramolecular Chemistry*, VCH, Weinheim, **1995**; b) J.-M. Lehn, *Struct. Bonding (Berlin)* **2000**, *96*, 3–29; c) G. M. Whitesides, B. Grzybowski, *Science* **2002**, *295*, 2418–2421; d) D. S. Lawrence, T. Jiang, M. Levett, *Chem. Rev.* **1995**, *95*, 2229–2260; e) M. M. Conn, J. Rebek, Jr., *Chem. Rev.* **1997**, *97*, 1647–1668; f) D. Philp, J. F. Stoddart, *Angew. Chem.* **1996**, *108*, 1242–1286; *Angew. Chem. Int. Ed. Engl.* **1996**, *35*, 1155–1196; g) M. Muthukumar, C. K. Ober, E. L. Thomas, *Science* **1997**, *277*, 1225–1232; f) L. J. Prins, D. N. Reinhoudt, P. Timmerman, *Angew. Chem.* **2001**, *113*, 2446–2492; *Angew. Chem. Int. Ed.* **2001**, *40*, 2382–2426.
- [2] For leading references on discotic liquid crystals, see: a) S. Chandrasekhar, G. S. Ranganath, *Rep. Prog. Phys.* **1990**, *53*, 57–84; b) C. Destradre, P. Foucher, H. Gasparoux, H. T. Nguyen, A. M. Levelut, J. Malthete, *Mol. Cryst. Liq. Cryst.* **1984**, *106*, 121–146; c) S. Chandrasekhar, S. Prasad, J. Krishna, *Contemp. Phys.* **1999**, *40*, 237–245; d) D. Guillon, *Struct. Bonding (Berlin)* **1999**, *95*, 41–82.
- [3] a) S. Chandrasekhar, B. K. Sadashiva, K. A. Suresh, *Pramana* **1977**, *9*, 471–480; b) S. Chandrasekhar, B. K. Sadashiva, K. A. Suresh, N. V. Madhusudana, S. Kumar, R. Shashidhar, G. Venkatesh, *J. Phys. Colloq.* **1979**, *3*, 120–124.
- [4] S. Chandrasekhar, *Handb. Liq. Cryst. Res.* **1998**, *2B*, 749–780.
- [5] a) N. Boden, B. Movaghar, *Handb. Liq. Cryst. Res.* **1998**, *2B*, 781–798; b) N. Boden, R. J. Bushby, J. Clements, B. Movaghar, *J. Mater. Chem.* **1999**, *9*, 2081–2086; c) A. M. Van de Craats, J. M. Warman, A. Fechtenkötter, J. D. Brand, M. A. Harbison, K. Müllen, *Adv. Mater.* **1999**, *11*, 1469–1472; d) V. Percec, M. Glodde, T. K. Bera, Y. Miura, I. Shiyonovskaya, K. D. Singer, V. S. Balagurusamy, P. A. Heiney, I. Schnell, A. Rapp, H.-W. Spiess, S. D. Hudson, H. Duan, *Nature* **2002**, *419*, 384–387; e) V. Percec, G. Johansson, J. Heck, G. Ungar, S. V. Batty, *J. Chem. Soc. Perkin Trans. 1* **1993**, 1411–1420; f) J. Simon, C. Sirlin, *Pure Appl. Chem.* **1989**, *61*, 1625–1629; g) O. E. Sielcken, L. A. van de Kuil, W. Drenth, J. Schoonman, R. J. M. Nolte, *J. Am. Chem. Soc.* **1990**, *112*, 3086–3093; h) T. Christ, B. Gluesen, A. Greiner, A. Kettner, R. Sander, V. Stuempflen, V. Tsukruk, J. H. Wendorff, *Adv. Mater.* **1997**, *9*, 48–52; i) D. Adam, P. Schuhmacher, J. Simmerer, L. Hänsling, K. Siemensmeyer, K. H. Etzbach, H. Ringsdorf, D. Haarer, *Nature* **1994**, *371*, 141–143; j) L. Schmidt-Mende, A. Fechtenkötter, K. Müllen, E. Moons, R. H. Friend, J. D. MacKenzie, *Science* **2001**, *293*, 1119–1122.
- [6] C. A. Hunter, J. K. M. Sanders, *J. Am. Chem. Soc.* **1990**, *112*, 5525–5534.
- [7] a) *Metallomesogens* (Ed.: J. L. Serrano), VCH, New York, **1996**; b) J. Simon, P. Bassoul in *Phthalocyanines: Properties and Applications, Vol. 2* (Eds.: C. C. Leznoff, A. B. P. Lever), VCH, New York, **1989**, chapter 6; c) A. G. Serrette, C. K. Lai, T. M. Swager, *Chem. Mater.* **1994**, *6*, 2252–2268.
- [8] V. Percec, *Handb. Liq. Cryst. Res.* **1997**, *2B*, 259–346.
- [9] a) M. Müller, C. Kubel, K. Müllen, *Chem. Eur. J.* **1998**, *4*, 2099–2109; b) H. Bengs, M. Ebert, O. Karthaus, B. Kohne, K. Praefcke, H. Ringsdorf, J. H. Wendorff, R. Wuestefeld, *Adv. Mater.* **1990**, *2*, 141–144; c) M. Weck, A. R. Dunn, K. Matsumoto, G. W. Coates, E. B. Lobkovsky, R. H. Grubbs, *Angew. Chem.* **1999**, *111*, 2909–2912; *Angew. Chem. Int. Ed.* **1999**, *38*, 2741–2745.
- [10] Hydrogen bonds used to stabilize π stacks: a) Y. Matsunaga, N. Miyajima, Y. Nakayasu, S. Sakai, M. Yonenaga, *Bull. Chem. Soc. Jpn.* **1988**, *61*, 207–210; b) L. Brunsveld, H. Zhang, M. Glasbeek, J. A. J. M. Vekemans, E. W. Meijer, *J. Am. Chem. Soc.* **2000**, *122*, 6175–6182, and references therein; c) Y. Yasuda, E. Iishi, H. Inada, Y. Shirota, *Chem. Lett.* **1996**, *7*, 575–576; d) M. P. Lightfoot, F. S. Mair, R. G. Pritchard, J. E. Warren, *Chem. Commun.* **1999**, *19*, 1945–1946; e) E. Fan, J. Yang, S. J. Geib, T. C. Stoner, M. D. Hopkins, A. D. Hamilton, *J. Chem. Soc. Chem. Commun.* **1995**, *12*, 1251–1252; f) D. Ranganathan, S. Kurur, R. Gilardi, I. L. Karle, *Biopolymers* **2000**, *54*, 289–295; g) C. M. Paleos, D. Tsiourvas, *Angew. Chem.* **1995**, *107*, 1839–1855; *Angew. Chem. Int. Ed. Engl.* **1995**, *34*, 1696–1711, and references therein; h) M. J. Brienne, J. Gabard, J.-M. Lehn, I. Stibor, *J. Chem. Soc. Chem. Commun.* **1989**, *24*, 1868–1870; i) D. Goldmann, R. Dietel, D. Janietz, C. Schmidt, J. H. Wendorff, *Liq. Cryst.* **1998**, *24*, 407–411; j) G. Ungar, D. Abramic, V. Percec, J. A. Heck, *Liq. Cryst.* **1996**, *21*, 73–86; k) V. Percec, C.-H. Ahn, T. K. Bera, G. Ungar, D. J. P. Yearley, *Chem. Eur. J.*

- 1999, 5, 1070–1083; l) J. Malthete, A. M. Levelut, L. Liebert, *Adv. Mater.* **1992**, 4, 37–41; m) D. Pucci, M. Veber, J. Malthete, *Liq. Cryst.* **1996**, 21, 153–155.
- [11] a) M. L. Bushey, A. Hwang, P. W. Stephens, C. Nuckolls, *J. Am. Chem. Soc.* **2001**, 123, 8157–8158; b) M. L. Bushey, A. Hwang, P. W. Stephens, C. Nuckolls, *Angew. Chem.* **2002**, 114, 2952–2955; *Angew. Chem. Int. Ed.* **2002**, 41, 2828–2831; c) T.-Q. Nguyen, M. L. Bushey, L. E. Brus, C. Nuckolls, *J. Am. Chem. Soc.* **2002**, 124, 15051–15054; d) W. Zhang, D. Horoszewski, J. Decatur, and C. Nuckolls, *J. Am. Chem. Soc.* **2003**, 125, 4870–4873; e) M. L. Bushey, T.-Q. Nguyen, C. Nuckolls, *J. Am. Chem. Soc.* **2003**, 125, 8264–8269.
- [12] a) D. Kilian, D. Knawby, M. A. Athanassopoulou, S. T. Trzaska, T. M. Swager, S. Wrobel, W. Haase, *Liq. Cryst.* **2000**, 27, 509–521; b) H. Zimmermann, R. Poupko, Z. Luz, J. Billard, *Z. Naturforsch. A* **1985**, 40, 149–160; c) J. Malthete, A. Collet, *J. Am. Chem. Soc.* **1987**, 109, 7544–7545.
- [13] a) B. Hueser, T. Pakula, H. W. Spiess, *Macromolecules* **1989**, 22, 1960–1963; b) S. Ikeda, Y. Takanishi, K. Ishikawa, H. Takezoe, *Mol. Cryst. Liq. Cryst. Sci. Technol. Sect. A* **1999**, 329, 1201–1207.
- [14] A. R. A. Palmans, J. A. J. M. Vekemans, R. A. Hikmet, H. Fischer, E. W. Meijer, *Adv. Mater.* **1998**, 10, 873–876.
- [15] Similar to the observation of mesogeneity in helicene liquid crystals: L. Vyklicky, S. H. Eichhorn, T. J. Katz, *Chem. Mater.* **2003**, 15, 3594–3601.
- [16] a) G. Gottarelli, E. Mezzina, G. P. Spada, F. Carsughi, G. Di Nicola, P. Mariani, A. Sabatucci, S. Bonazzi, *Helv. Chim. Acta* **1996**, 79, 220–234, and references therein; b) A. R. A. Palmans, J. A. J. M. Vekemans, E. E. Havinga, E. W. Meijer, *Angew. Chem.* **1997**, 109, 2763–2765; *Angew. Chem. Int. Ed. Engl.* **1997**, 36, 2648–2650; c) S. T. Trzaska, H.-F. Hsu, T. M. Swager, *J. Am. Chem. Soc.* **1999**, 121, 4518–4519; d) C. F. van Nostrum, A. W. Bosman, G. H. Gelinck, P. G. Schouten, J. M. Warman, A. P. M. Kentgens, M. A. C. Devillers, A. Meijerink, S. J. Picken, U. Sohling, A.-J. Schouten, R. J. M. Nolte, *Chem. Eur. J.* **1995**, 1, 171–182; e) H. Engelkamp, C. F. van Nostrum, R. J. M. Nolte, S. J. Picken, *Chem. Commun.* **1998**, 9, 979–980.
- [17] A. A. Kornyshev, S. Leikin, *Phys. Rev. E* **2000**, 62, 2576–2596, and references therein.
- [18] DNA and nucleic acid derivatives: a) F. Livolant, A. M. Levelut, J. Doucet, J. P. Benoit, *Nature* **1989**, 339, 724–726; b) K. Merchant, R. L. Rill, *Biophys. J.* **1997**, 73, 3154–3163; c) R. L. Rill, F. Livolant, H. C. Aldrich, M. W. Davidson, *Chromosoma* **1989**, 98, 280–286; d) G. Gottarelli, G. Proni, G. P. Spada, S. Bonazzi, A. Garbesi, F. Ciuchi, P. Mariani, *Biopolymers* **1997**, 42, 561–574; e) G. Proni, G. Gottarelli, P. Mariani, G. P. Spada, *Chem. Eur. J.* **2000**, 6, 3249–3253.
- [19] In polypeptides: a) D. B. DuPré, E. T. Samulski in *Liquid Crystals—The Fourth State of Matter* (Ed.: F. D. Saeva), Marcel Dekker, New York, **1979** chapter 5; b) T. Hashimoto, S. Ebusu, N. Inaba, H. Kawai, *Polym. J.* **1981**, 13, 701–713.
- [20] a) X. M. Dong, D. G. Gray, *Langmuir* **1997**, 13, 3029–3034; b) T. Sato, J. Nakamura, A. Teramoto, M. M. Green, *Macromolecules* **1998**, 31, 1398–1405.
- [21] T. Sato, Y. Sato, Y. Umemura, A. Teramoto, Y. Nagamura, J. Wagner, D. Weng, Y. Okamoto, K. Hatada, M. M. Green, *Macromolecules* **1993**, 26, 4551–4559.
- [22] *Liquid Crystals—The Fourth State of Matter* (Ed.: F. D. Saeva), Marcel Dekker, New York, **1979**.
- [23] W. Cao, A. Munoz, P. Palffy-Muhoray, B. Taheri, *Nat. Mater.* **2002**, 1, 111–113.
- [24] J. S. Moore, *Curr. Opin. Colloid Interface Sci.* **1999**, 4, 108–116.
- [25] EFM theory and experimental setup: a) T. D. Krauss, S. O'Brien, L. E. Brus, *J. Phys. Chem. B* **2001**, 105, 1725; b) J. Jiang, T. D. Krauss, L. E. Brus, *J. Phys. Chem. B* **2000**, 104, 11936–11941; c) O. Cherniavskaya, L. Chen, V. Chen, L. Yuditsky, L. E. Brus, *J. Phys. Chem. B* **2003**, 107, 1525–1531.
- [26] Similar to the recognition of carbon nanotubes with amines: a) J. Liu, M. J. Casavant, M. Cox, D. A. Walters, P. Boul, W. Lu, A. J. Rumberg, K. A. Smith, G. T. Colbert, R. E. Smalley, *Chem. Phys. Lett.* **1999**, 303, 125–129; b) M. J. O'Connell, P. Boul, L. M. Ericson, C. Huffman, Y. Wang, E. Haroz, C. Kuper, J. Tour, K. D. Ausman, R. E. Smalley, *Chem. Phys. Lett.* **2001**, 332, 461–466; c) J. Kong, H. Dai, *J. Phys. Chem. B* **2001**, 105, 2890–2893; d) M. Sano, A. Kamino, J. Okamura, S. Shinkai, *Nano Lett.* **2002**, 2, 531–533.
- [27] Surface poling has been observed locally in polymer films: X. Q. Chen, H. Yamada, Y. Terai, T. Horiuchi, K. Matsushige, P. S. Weiss, *Thin Solid Films* **1999**, 353, 259–263.
- [28] J. J. van Gorp, J. A. J. M. Vekemans, E. W. Meijer, *J. Am. Chem. Soc.* **2002**, 124, 14759–14769.
- [29] a) P. Henderson, D. Beyer, U. Jonas, O. Karthaus, H. Ringsdorf, P. A. Heiney, N. C. Maliszewskij, S. S. Ghosh, O. Y. Mindyuk, J. Y. Josefowicz, *J. Am. Chem. Soc.* **1997**, 119, 4740–4748; b) N. C. Maliszewskij, P. A. Heiney, J. Y. Josefowicz, J. P. McCauley, Jr., A. B. Smith III, *Science* **1994**, 264, 77–79; c) J. Y. Josefowicz, N. C. Maliszewskij, S. H. J. Idziak, P. A. Heiney, J. P. McCauley, Jr., A. B. Smith III, *Science* **1993**, 260, 323–326; d) V. V. Tsukruk, D. H. Reneker, H. Bengs, H. Ringsdorf, *Langmuir* **1993**, 9, 2141–2144; e) T. Christ, F. Geffarth, B. Glösen, A. Kettner, G. Lüssem, O. Schäfer, V. Stümpflen, J. H. Wendorff, V. V. Tsukruk, *Thin Solid Films* **1997**, 302, 214–222.
- [30] For leading references on foldamers see: a) R. P. Cheng, S. H. Gellman, W. F. DeGrado, *Chem. Rev.* **2001**, 101, 3219–3232; b) D. J. Hill, M. J. Mio, R. B. Prince, T. S. Hughes, J. S. Moore, *Chem. Rev.* **2001**, 101, 3893–4011; c) D. Seebach, A. K. Beck, M. Rueping, J. V. Schreiber, H. Sellner, *Chimia* **2001**, 55, 98–103.